Chalcogenide Letters Vol. 8, No. 3, March 2011, p.171 – 176

LUMINESCENCE PROPERTIES OF ZnS QUANTUM DOTS EMBEDDED IN POLYMER MATRIX

BIJOY BARMAN*, K. C. SARMA
Department of Instrumentation and USIC, Gauhati University, Guwahati - 781014, Assam, India

Zinc Sulfide (ZnS) quantum dots of sizes 2.68-4.8 nm, embedded on polyvinyl alcohol (PVA) matrix, have been synthesized at 70^0C by chemical route. X-ray diffraction (XRD), High Resolution Transmission Electron Microscopy (HRTEM), Scanning Electron Microscopy (SEM), UV-VIS Spectroscopy and Photoluminescence (PL) Spectroscopy has been adopted for sample characterization. Optical absorption spectra showed strong blue shift, which is an indication of strong quantum confinement. Photoluminescence spectra of the sample have been recorded at room temperature and observed two peaks centred around 415 nm and 440 nm. We have assigned the first peak due to band gap transitions while the later due to sulfur vacancy in the sample.

(Received February 5, 2011; accepted February 14, 2011)

Keywords: Zinc Sulfide, Quantum dots, Blue shift, Luminescence

1. Introduction

Zinc Sulfide (ZnS) is a II-VI semiconductor with direct band gap of 3.68 eV at room temperature [1]. It is considered as an important material for the preparation of semiconductor quantum dots and their application in electronics, optoelectronics, magnetic and non linear optics are the frontier area of research [2-6]. ZnS quantum dots can be obtained by different techniques, such as screen printing [7], electro deposition [8], molecular beam epitaxy (MBE) [9], physical vapour deposition [10] etc. All these techniques require highly sophisticated instrument and mismatch of thermal expansion coefficient between the film and substrate causes micro cracks. Keeping all these aspects in view, we have carried out a systematic study on the optical properties of ZnS quantum dots in polymer host polyvinyl alcohol in the regime of strong confinement by chemical process [11]. Luminescence measurements are identified as one of the most important techniques to reveal the energy structure and surface state of these particles [12]. UV-VIS absorption spectroscopy reveals strong blue shift of absorption edge which gives a clear indication of the formation of quantum dots [13]. Localized trap state inside the band gap recognizes the sub band gap energy level [14]. The defect level plays an important role in determining the luminescence characteristics of the ZnS quantum dots [15]. The present study is aimed to synthesize nanoparticles of ZnS and their optical studies by optical absorption and photoluminescence spectroscopy (PL). X-ray diffraction (XRD), high resolution transmission electron microscopy (HRTEM) and scanning electron microscopy (SEM) have also been carried out to verify the formation of ZnS quantum dots.

2. Experimental

ZnS nanocrystalline thin films were synthesized using polyvinyl alcohol (PVA) as a matrix by an ion exchange reaction. PVA being a good solute to multiple phase system,

*Corresponding author: bb_ guphys@rediffmail.com

it provides uniform gaps that are very close to each other and distributes in the form of array. 2 wt% solutions of PVA was mixed with various concentration of $ZnCl_2$ (0.75M, 1M) under a high stirring rate (200rpm) condition using magnetic stirrer. The constant temperature 70^0 C for 3 hours was maintained during the process of stirring. The sample under preparation was kept for 12 hours for complete dissolution to get a transparent solution. An equimolar solution of Na_2S was added drop by drop to this solution, until it appears completely milky. The prepared samples were kept overnight for stabilisation and were cast over a glass substrate for characterization.

3. Results and discussion

3.1. XRD measurements

ZnS quantum dots were synthesized in the polymer matrix by an ion exchange reaction as discussed in the experimental details. The XRD patterns of prepared samples were taken by Seifert XRD (3003TT) operating at 40KV-30mA. Fig 1. shows the XRD patterns of ZnS thin films of various concentrations (1M, 0.75M). The three broad peaks observed in the diffractogram at around 28.58^o, 48.29^o and 56.17^o for 1M and 28.61^o, 47.96^o and 56.31^o for 0.75M reveals a cubic lattice structure of ZnS (Zincblende). These peaks could be easily assigned to the planes (111), (220) and (311) respectively of the cubic phase [16]. The peak broadening in the XRD patterns clearly indicates the formation of ZnS nanocrystal of small size.

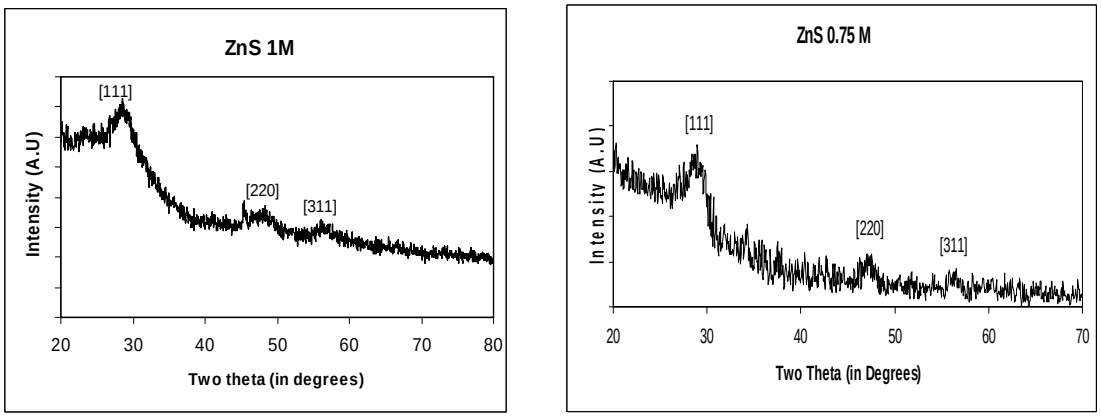

Fig 1. XRD patterns of ZnS Thin films.

The increase in diffraction angle is clearly a result of lattice contraction expected to occur because of higher surface to volume ratio [17]. From X-ray diffraction study, average particle size has been calculated by using Debye Scherrer formula [18].

$$D= K\lambda/\beta_{2\theta}\cos\theta. \quad (1)$$

where θ is the Bragg angle and λ is the X-ray wavelength. Here K=0.89 for spherical shape (evidence from TEM). For calculation $\beta_{2\theta}$ is observed by zooming the peak position using origin graphic software. The calculated size is found to be 4.05 nm for 0.75M and 3.80 nm for1M (table 1).

3.2. Optical Absorption

Optical absorption spectra of the ZnS sample were measured using a HITACHI-U 3210 UV-VIS spectrometer. Fig 2. shows the absorption spectra of the ZnS quantum dots.

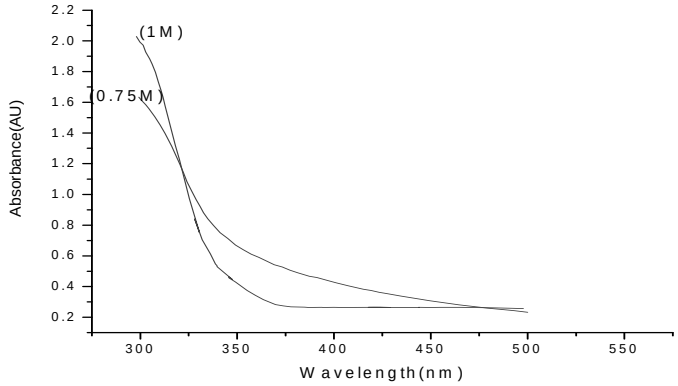

Fig 2. Absorption spectra of ZnS quantum dots.

It is clear from Fig 2 that the samples exhibit absorption edges which are blue shifted with decreasing particle size. This blue shift of the absorption edges for nanocrystals arises from quantum confinement effect in the nanoparticles. The band gap of the sample were determined using the relation,

$$(\alpha h\upsilon) = C\,(h\upsilon - Eg)^n \qquad (2)$$

where C is a constant, Eg is the band gap of the material and exponent n depends on the type of transition [19], for direct transition we take n=1/2. The value of the optical band gap is calculated by extra plotting the straight line portion of $(\alpha h\upsilon)^2$ vs. $h\upsilon$ graph (Fig. 3) to $h\upsilon$ axis. The obtained band gap values of the sample are 3.96 eV (0.75M) and 4.06 eV (1M) which are blue shifted as compared to the bulk band gap value and is the evidence of the effect of quantum confinement in the ZnS quantum dots.

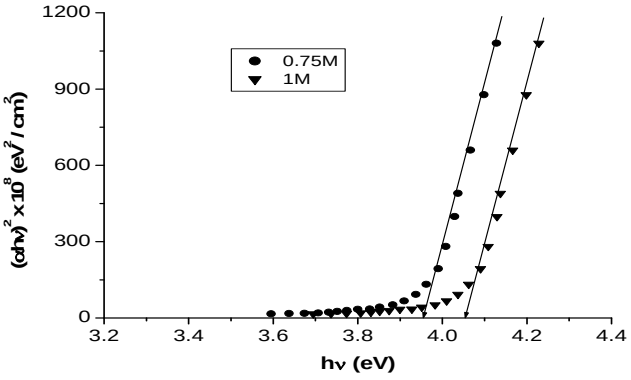

Fig 3. Band gap determination of ZnS quantum dots.

The shift of in the band gap might also be utilized in determining the quantum dot size (d_g) using the effective mass approximation relation [20,21,22]

$$\Delta E_g = E_g\,(\text{film}) - E_g\,(\text{bulk}) = h^2/8\mu d_g^2 - 1.8e^2/\epsilon d_g \qquad (3)$$

where $1/\mu = 1/m_e^* + 1/m_h^*$ is the effective mass of electron and hole. For cubic ZnS, $m_e^* = 0.34m_o$ and $m_h^* = 0.23m_o$ and ϵ (= 8.76) is the permittivity of the sample. The particle size obtained from this equation nearly matches that estimated from XRD and is shown in table 1.

Table 1. Variation of particle size and energy band gap of ZnS quantum dots.

Molarity	Particle size from XRD (nm)	Particle size from TEM (nm)	Energy band gap (eV)	Blueshift (eV)	Particle size from EMA (nm)
0.75 M	4.05	4.8	3.96	0.28	3.12
1.0 M	3.80	2.8	4.06	0.38	2.68

3.3. Photoluminescence (PL)

The photoluminescence spectra of ZnS quantum dots embedded in PVA matrix are shown in Fig 4. The spectra were recorded using (F 2500) FL spectrometer with an excitation wavelength 368 nm.

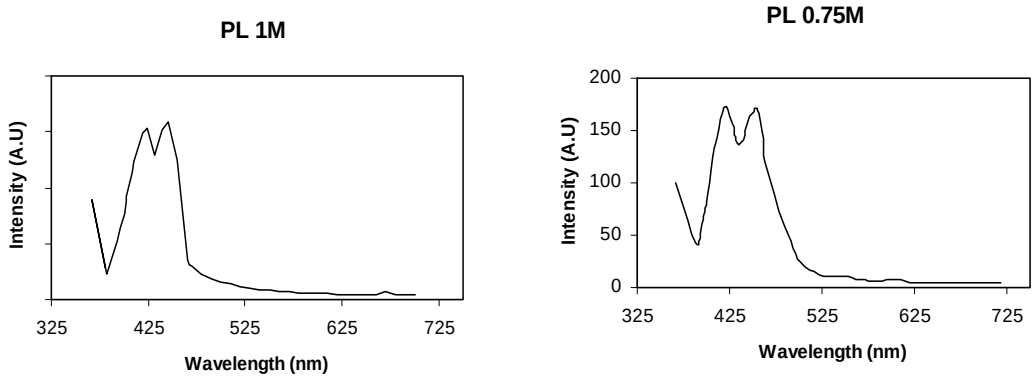

Fig 4. PL spectra of ZnS quantum dots.

In Fig 4, two well resolved peaks are observed. The peak positioned around 415 nm and 440 nm are due to the shallow state near the conduction band and the sulphur vacancies present near the valance band [23]. It is observed that the photoluminescence efficiency of ZnS quantum dot containing PVA matrix is higher than that of the powder samples due to passivation of surfaces [24]. The blue emission at 415nm is attributed to sulphur vacancies[25] and the emission peak at 440 nm is attributed to the zinc vacancies which is quite agree as reported by other workers [26,27].

3.4. Scanning electron microscopy (SEM)

The thin film sample containing PVA were coated with a thin layer of Gold (Au) by sputtering and their micro structure were observed using a scanning electron microscope (HITACHI S-530) operated at an accelerating voltage of 20 kV.

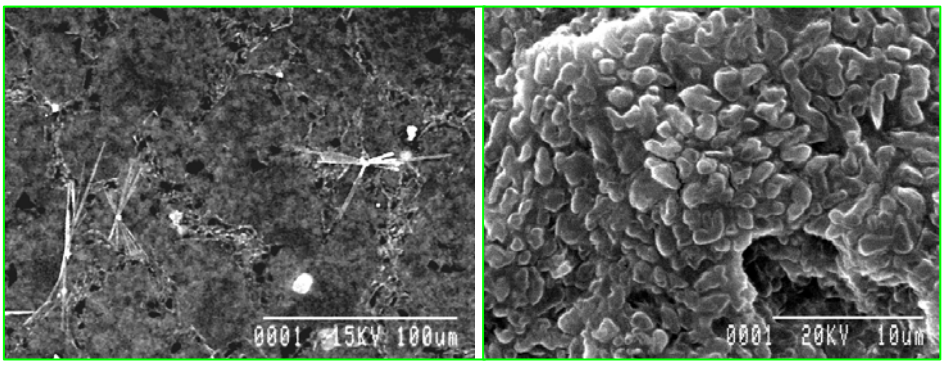

Fig 5. SEM image of ZnS quantum dots.

Scanning electron microscope is a convenient technique to study the microstructure of the film. Fig.5, shows that the films are homogeneous, without any crack and exhibit almost complete coverage of the substrates. The distributions of grains are of irregular shape through all the regions. So for the optoelectronic observations, the qualities of such grown films are quite suitable.

3.5. Transmission electron microscopy (TEM)

Transmission electron microscopy (TEM) image was obtained using a JEOL JEM 2100 electron microscope operated at 200 KV.

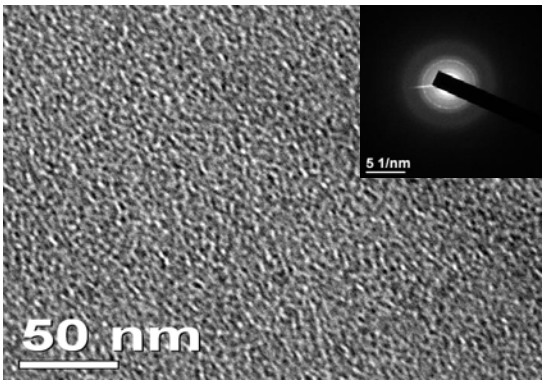

Fig 6. TEM image of ZnS quantum dots.

HRTEM image of the ZnS 1M sample shown in Fig 6 indicates the nanocrystalline nature of the sample with distinct grain boundaries having average crystallite size of 2.8 nm. The nanoparticles have also seen to be of more or less spherical shape with clear lattice fringes showing the well crystallized particles. The inset image is the selected area electron diffraction pattern corresponding to the image. All of them show three rings that can be indexed to (111), (220), and (311) lattice planes of cubic ZnS [28]. The size is also nearly consistent with the size obtained from XRD observations.

4. Conclusions

Nanosized ZnS quantum dots have been successfully synthesized by chemical route in PVA matrix. X-ray diffraction patterns and selected area electron diffraction patterns confirmed the nanocrystalline cubic ZnS phase formation. TEM micrographs of the samples revealed the manifestation of ZnS quantum dots with size within the range of 2.68-4.8 nm. UV-VIS spectrophotometric measurement and PL studies of the sample clearly show an increase in band gap which supports the formation of nanocrystallites. It, therefore, shows that the ZnS quantum dots exhibit strong quantum confinement effect as the optical band gap increases significantly, from 3.96 eV to 4.06 eV, compared to bulk value 3.68 eV. The particle sizes calculated from the shift of direct band gap and XRD are also well matched with TEM results.

Acknowledgements

The authors acknowledge Department of Physics and CIF, IIT'G for providing XRD and TEM facilities and USIC, Burdwan University, West Bengal for providing SEM observation. They also acknowledge Department of Chemistry, Gauhati University for spectrometer observation.

References

[1] N. Kumbhojkar, V. V. Nikesh, A. Kashirsagar, S. Mahamuni, J. Appl. Phys. **88,** 6260 (2000)
[2] L. Brus, Appl. Phys. A, Solid Surf. **53**, 465 (1991)
[3] C. K. Rasyogi, C. S. Kumbhakar and A. K. Misra, Asian J. Chem. **21**, S039 (2009)
[4] B. L. Zhu, X. Chen, Z. M. Sui, L. M. Xu, C. J. Yang, J. K. Zhao, J. Liu, Chinese Chem. Lett. **15**, 97 (2004)
[5] P. K. Kalita, B. K. Sarma, H. L. Das, Bull. Mater. Sci. **26**, 613 (2003)
[6] A. Zdyb, K. Cieslak, J. M. Olchowik, Materials Science Poland **26**, 389 (2008)
[7] H. E. Ruda, Wide gap II-VI Compound for optoelectronic applications, Chapman and Hall, London (1992)
[8] S. Kar and S. Chaudhuri, J. Phys. Chem. B **110**, 4542 (2006)
[9] P. Vasa, P. Ayyub and B. P. Sing, Appl. Phys. Lett. **87**, 063104 (2005)
[10] A. Mews, A. V. Kadavanich, U. Banin and A. P. Alivisator, Phys. Rev. B **53**, 242 (1996)
[11] J. Barman. J. P. Borah and K. C. Sarma, International Journal of Modern Phys B **23**, 545 (2009)
[12] W. Chen, Z. Wang, Z. Lin, L. Lin, J. Appl. Phys. **82**, 3111 (1997)
[13] S. Nath, D. Chakdar, G. Gope and D. K. Avasti, International Journal of Nanotechnology and Application **2**, 47 (2008)
[14] D. Denzler, M. Olschewski, K. Sattler, J. Appl. Phys. **84**, 2841 (1998)
[15] K. Kanemoto, H. Hosokawa, Y. Wada, K. Murakoshi, S. Yanagida, T. Sakata, H. Mori, M. Isikawa, H. Kobayashi, J. Chem. Soc. Faraday Trans **92**, 2401 (1996)
[16] R. Sahraei, G. M. Aval, A. Baghizadeh, M. L. Rachti, A. Goudarzi, M. H. Majles Ara, Materials Letters **62**, 4345 (2008)
[17] K. K. Nanda, S. N. Sarangi and S. N. Shu, Nanostructures Material **10**, 1401 (1998)
[18] H. P. Klug and L. E. Alexander, X-ray Diffraction Procedures. John Willy and Sons, Inc. New York (1954), Chapter 9, p 512.
[19] G. P. Joshi, N. S. Saxena, T. P. Sharma, V. Dixit and S.C.K Mishra, Ind. J. Pure. Appl. Phys. **41**, 462 (2003)
[20] A. D. Yoffe, Adv. Phys. **42**, 173 (1993)
[21] Y. S. Yuang, F. Y. Chen, Y. Y. Lee, C. L. Liu, Jpn. J. Appl. Phys. **76**, 304 (1994)
[22] P. K. Ghosh, S. Jana, S. Nandy, K. K. Chattopadhyay, Material Research Bulletin **42**, 505 (2007)
[23] J. Nanda, D. D. Sarma, J. Appl. Phys. **90**, 2504 (2001)
[24] R. N. Bhargava and D. Gallagher, Phys. Rev. Lett. **72**, 416 (1994)
[25] P. V. B. Lakshmi, K. S. Raj and K. Ramachandran, Cryst. Res. Technol. **44**, 153 (2009)
[26] N. Murase, R. Jagannathan, Y. Kanematsu, M. Watanabe, A. Kurita, H. Hirata, T. Yazawa, T. Kushida, J. Phys. Chem. B **103**, 754 (1999)
[27] S. Wageh, Z. S. Ling, X. X. Rong, J. Cryst. Growth **255**, 332 (2003)
[28] S. Liu, H. Zhang, M. T. Swihart, Nanotechnology **20**, 235603 (2009)